SUPPLEMENTAL DISCUSSION

The Herringbone ^{HB}CTC-Chip used in this paper has been reported as a technology to enrich for CTCs from epithelial cancers (eg. breast, prostate and lung) (Stott et al., 2010) and the current studies extend its application to melanoma, which express different and more heterogeneous cell surface antigens than most epithelial cancers. While these proof of principle experiments provide insight into the biology of melanoma metastasis, the ^{HB}CTC-Chip platform is not sufficiently robust for routine clinical application in patients with metastatic melanoma. Ongoing work is aimed at developing a robust, clinical grade platform for tumor-epitope independent CTC capture (Ozkumur et al., 2013).

SUPPLEMENTAL EXPERIMENTAL PROCEDURES

Mouse tumor tissue and cell line. The mouse melanoma cell line was generated from the established B-RAF$^{V600E/+}$; PTEN$^{-/-}$ tumor following collagenase IV (Sigma) digestion. Cells suspended in PBS were deposited onto a microscopic slide by Cytospin (Thermo Scientific) and stained with antibodies against CSPG4 (R&D Systems, Clone LHM-2) and MCAM (Miltenyi Biotec, Clone LSEC). The immunofluorescent (IF) staining procedures for mouse melanoma FFPE sections are listed as the following. Briefly, paraffin-embedded mouse melanoma sections were deparaffinized followed by heat mediated antigen retrieval (50mM Tris-HCl pH9.0, 100 °C for 20 minutes). After blocking with 1%BSA-PBS, the slides were incubated with primary antibodies (rabbit anti-S100, DAKO, 1:400; mouse anti-GP100, clone HMB45, Santa Cruz, 1:200) in blocking solution (1%BSA and 0.1% Triton-X in PBS) overnight at 4°C. Secondary antibodies used were goat anti-mouse Alexa Fluor 488(Invitrogen, 1:500) and goat anti-rabbit Alexa Fluor 594 (Invitrogen, 1:500). Nuclei were counter-stained with Hoechst (1:20000 in PBS). Images were taken on a fluorescent microscope (Nikon Eclipse 90i).

Mouse tumor induction and *in vivo* PLX study. All the animal procedures were approved by the MGH Subcommittee on Research Animal Care (SRAC). The *B-raf*$^{CA/+}$*/Pten* $^{flox/flox}$*/Tyr-CreER* mouse was described previously (Dankort et al., 2009) and was backcrossed into C57BL/6 genetic background. For tumor induction, the mice received either 1) focal subcutaneous injection of regular tamoxifen (Sigma T5648) (50ul at 5mg/ml in 50% EtOH suspension) at the flank (Figure 1) at 6-7 weeks after birth or 2) topical application of the active

metabolite of tamoxifen, 4-hydroxytamoxifen, 4-HT, (1ul at 20mg/ml in 100% EtOH) (Sigma H7904) at the left ear (Figure 2) at 24-27 days after birth. For subcutaneous injection-induced tumors, the mice were sacrificed at day 7, 14, 21, 28, 35 or 56 for CTC analysis (Figure 1, S1). In mice with ear tumors, the mice were sacrificed at day 7, 14, 21 and 28 to enumerate their CTCs (Figure 2). Corresponding tumor specimens were collected at the necropsy and immediately fixed with 4% formaldehyde.

In the mouse ear tumor surgery model, the 4-HT treated ears were surgically removed at day 4, 7, 14, 21 or 28 after tumor induction. Buprenex was given at 0.1mg/kg for each mouse 30 minutes prior to the surgery followed by 2 more doses at 12 and 24 hours post-procedure. All ear samples were immediately fixed (4% formaldehyde) and paraffin embedded. Tumors were graded and surgical margins were determined free of tumor cells by a Board-certified pathologist (negative surgical margins not obtained from day 21 and 28 tumors due to tumor progression).

For *in vivo* PLX4720 study, animals were given mouse chow containing 417mg/kg (Figure 1, S1), 200mg/kg PLX4720 (Plexxikon) (Figure S1) or control chow. For mice that received tamoxifen injection, special diets were given at post-injection day 28 for 4, 7 (Figure 1) or 14 days (Figure S1) until sacrifice. For mice that received 4-HT ear application, special food was given post-operatively for 4 weeks.

Mouse blood processing, CTC staining and enumeration. ^{HB}CTC-Chips were manufactured as previously described (Stott et al., 2010). Mouse ^{HB}CTC-Chips were functionalized with biotinylated anti-CSPG4 (R&D, Clone LHM-2) and anti-MCAM (Miltenyi Biotec, Rat IgG, Clone LSEC) for CTC capture or isotype control biotinylated mouse IgG1 and Rat IgG (BioLegend).

For mouse blood processing, approximately 0.9-1ml of blood was collected from each mouse by cardiac puncture and immediately diluted 1:1 with PBS-10mM EDTA pH 7.4. About one milliliter of diluted blood was subsequently processed through the chip using a syringe pump (Harvard Apparatus) at 1.25ml/hr followed by PBS flush (Yu et al., 2012) followed by either 4% paraformaldehyde fixation or RNA extraction.

For IF staining of mouse ^{HB}CTC-chips, following the blood run, cells that remained on the chip were fixed with 4% paraformaldehyde, permeabilized with 1% NP-40 in PBS and blocked with 3%BSA/2% donkey serum in PBS. Primary antibodies for in-line staining of mouse ^{HB}CTC-chips were anti-CD45 (R&D Systems, goat, 1:500) and anti-S100 (DAKO, rabbit, 1:400). Secondary antibodies were donkey anti-goat Alexa Fluor 488 (Invitrogen, 1:500) and donkey anti-rabbit Alexa Fluor 594 (Invitrogen, 1:500). Nuclei were stained with DAPI (Invitrogen, 1:1000). The chips were automatically imaged using the BioView imaging system (BioView Ltd.) at 10x magnification followed by automated imaging at 40x (BioView) or 60x magnification (Nikon Eclipse 90i). Cells positive for CTC markers but not CD45 were scored as potential CTCs and were subsequently subject to manual review. Detection baselines were determined based on specimen from three types of tumor-free mice including a) genotype-matched un-induced mice (n = 8), b) mice carrying *B-raf* $^{CA/+}$/*Pten* $^{flox/flox}$ but lacking the critical *Tyr-CreER* that received subcutaneous injection of tamoxifen (n = 5) and c) syngeneic C57BL/6 mice (n = 9) (purchased from the Jackson Laboratory). CTC counts were presented as CTCs per milliliter of whole blood.

RNA extraction and single molecule sequencing. Eight weeks after tamoxifen injection, blood samples were collected from mice (n = 5) with very high tumor burden, split and processed through the ^{HB}CTC-chips functionalized with anti-CSPG4/MCAM antibody and control IgGs, respectively. Matched primary (from the tamoxifen injection site) and metastatic (from upper or lower back) tumors were harvested from the same mouse and immediately flash-frozen in liquid nitrogen.

RNA extraction and single molecular sequencing was described previously (Yu et al., 2012). Briefly, RNA from fresh frozen tumor tissues was extracted using RNeasy MiniElute kit (Qiagen). RNA from Chip-captured cells was extracted and purified using RNeasy MicroKit (Qiagen) followed by cDNA synthesis using SuperScript III kit (Invitrogen). cDNAs were then poly-A tailed at the 3' end and subject to single molecule sequencing (Helicos Biosciences).

Bioinformatics analysis. Digital Gene Expression (DGE) analysis is performed as previously described (Yu et al., 2012). For unsupervised clustering analysis, we excluded all genes with any reads in the mock (IgG) control ^{HB}CTC-Chip and all genes with no reads in the CTC, primary or metastasis. The log(reads) of the genes with the 1000 highest standard deviation were submitted to average linkage agglomerative hierarchical clustering with distance defined as 1 – correlation coefficient. The DGE profiles were compared as previously described (Yu et al., 2012) with threshold for statistical significance a Benjamini–Hochberg q-value of 10^{-5} and a fold-change threshold of 2. Hypergeometric gene set enrichment analysis (hGSEA) was done as previously described (Yu et al., 2012) using genes sets obtained from MSigDB v 3.0 (Broad Institute) with an FDR threshold of 10%. Metagene values were computed as the mean log2(expression) (Fig 3F) or expression (Fig 3G) for all the genes in the gene set. If multiple rows of the expression matrix mapped to the same gene, the row with the maximum standard deviation was used. P-values for trends in metagene values were computed by the Wilcoxon test (Fig. 3F) or the likelihood ratio test applied to the cumulative link model with logit link function as implemented in version 2012.09-11 of the R-project package "ordinal" (Fig 3G).

Human cell lines, flowcytometry and IF staining. Human melanoma cell lines were cultured in RPMI-1640 media with 10% fetal bovine serum (FBS) and 1% Pen/Strep. SK-MEL-28 and MeWo were purchased from ATCC. 501MEL, M14, MALME-3M, SK-MEL-2, SK-MEL-5, UACC62 were a gift from Dr. David E. Fisher. SK-MEL-3, HT-144 and WM266-4 were a gift from Dr. Cyril Benes.

Cultured melanoma cells were dissociated from plates using either Accutase (eBioscience) or enzyme-free cell dissociation buffer (GIBCO). Cells were re-suspended and blocked in 1%BSA/1%FBS-PBS for 20min and subsequently stained with either primary antibody or isotype control in blocking buffer for 30min at 4°C. Alexa Fluor 647-conjugated secondary antibodies were used to amplify the signal. After washing, each sample was re-suspended and post-fixed with 500ul of 1% paraformaldehyde before being analyzed on a cytometer (BD LSRII). For IF staining, cells were fixed (4% paraformaldehyde), permeabilized (1% NP-40-PBS) and blocked (3% BSA-PBS) prior to antibody incubation.

Patient ^{HB}CTC-Chip optimization and blood specimen processing. For human ^{HB}CTC-Chip optimization, efficiency of cell capture was determined using pre-labeled (Celltracker Orange, Invitrogen), defined numbers of cancer cells spiked into control blood and processed through ^{HB}CTC-Chip. Cancer cell capture efficiency was calculated based on the number of cells retained on the ^{HB}CTC-Chip versus the number of cells that ran through the chip.

^{HB}CTC-Chips for patient specimens were functionalized with biotinylated antibodies against 12 human melanoma antigens (Table S4). The most critical antibodies for successful melanoma CTC capture targeted CSPG4 (present on 8 out of 11 human melanoma cell lines), p97/melanotransferrin (8 out of 10) and MCAM (8 out of 11) epitopes (X.L. and D.H., unpublished data), which in combination allowed ^{HB}CTC-Chip capture of cultured SK-MEL-28 cell with >90% efficiency (Figure S4). The additional nine antibodies (Table S4) were derived from pairwise comparisons and optimization using clinical specimens, and together, their inclusion increased the number of patient melanoma CTCs captured by up to five-fold. In brief, anti-CSPG4 (mouse IgG1, Clone LHM-2), EphA2 (goat), c-Met (goat) and A2B5 (mouse IgM) were from R&D Systems. Anti-MCAM (mouse IgG1, Clone P1H12) and NGFR (mouse IgG1, Clone NGFR5) were purchased from Abcam. Anti-c-kit (mouse IgG1, Clone 104D2), CD90 (mouse IgG1, Clone 5E10) and HNK-1 (mouse IgM) were obtained from BioLegend. Anti-N-Cadherin (mouse IgG1, Clone 8C11) was from eBioscience. Cetuximab (ImClone), a chimeric antibody against human EGFR, was biotinylated in house. Anti- p97/melanotransferrin (mouse IgG1, Clone L235) was purified from the culture supernatant of a hybridoma cell line (ATCC, HB-8446) and biotinylated by Covance.

In-patients with metastatic melanoma were enrolled according to an institutional review board, IRB, approved protocol (05-300). Blood samples from healthy volunteers were collected under a separate IRB-approved protocol. All blood specimens were collected between 8am and 2pm. All blood samples from the same patient were collected within the same 2-hour window across multiple appointment dates.

All human blood specimens were processed as described previously (Stott et al., 2010). In brief, patient blood samples were collected into vacutainer tubes (BD) and processed through ^{HB}CTC-

Chip within 4 hours of blood draw. About 2.5ml of blood was driven through the chip using the microfluidic-processing machine described previously (Stott et al., 2010) at a flow rate of 1.25ml/hr followed by a 2.5ml of PBS flush at 2.5ml/hr. 4% paraformaldehyde was subsequently delivered to the ^{HB}CTC-chips to fix the retained cells.

Patient CTC staining and enumeration. Primary antibodies for human ^{HB}CTC-chips IF staining were anti-CSPG4 (Abcam, mouse IgG2a, Clone 9.2.27, 1:100), anti-MCAM (BioLegend, mouse IgG2a, Clone SHM-57, 1:200), anti-TYRP1 (Abcam, mouse IgG2a, Clone TA99, 1:200), anti-αSMA (Sigma, mouse IgG2a, Clone 1A4, 1:400) and anti-CD45 (Santa Cruz, Rat IgG, Clone 3H1363, 1:400). The antibodies against MCAM and CSPG4 used in CTC IF staining were distinct from those used as capture antibodies (Table S4). Secondary fluorescent-conjugated antibodies were goat anti-mouse IgG2a Alexa Fluor 594 (Invitrogen, 1:500) and goat anti-Rat Alexa Fluor 488 (Invitrogen, 1:500). Human ^{HB}CTC-Chips were imaged the same way as for mouse chips. Detection threshold was set based on specimens from healthy volunteers. In all cases, CTCs were scored blind without prior knowledge of clinical history.

Patient tumor assessment was performed using Response Evaluation Criteria in Solid Tumors (RECIST) from restaging imaging performed every 6-8 weeks.

SUPPLEMENTAL FIGURES

Figure S1: Characterization of the mouse melanoma CTC model. (A-D) Marker expression in mouse melanomas. (A and B) IF staining of tumor-derived cell line demonstrated the expression of CSPG4 (A) and MCAM (B). (C and D) IF staining of tumor sections revealed the expression S100 (C) and GP100 (D) in tumor cells (asterisk, epidermis; arrowheads, basal layer; arrow, tumor). (E) CTC numbers correlate with tumor progression. Number of CTCs increase significantly after tumor initiation. (F) Mouse melanoma responded to selective B-RAF inhibitor PLX4720 showing dramatic tumor shrinkage as early as 4 days after treatment initiation (see main text for tumor volume quantification). (G-H) Prolonged PLX4720 exposure reduces CTC counts in a dose-dependent manner. (G) Representative images of mice on control chow (top panel) or 417mg/kg PLX4720 chow (bottom panel) for 2 weeks. (H) CTCs responded to B-RAF inhibitor in a dose-dependent manner (blue squares, CTCs from mice on control diet; pink diamonds, CTCs from mice fed with 200mg/kg PLX4720; red triangles, CTCs from mice fed with 417mg/kg PLX4720).

Figure S2: Surgery alone does not lead to a cure of early melanoma in mice. Ear was resected at day 7, 14, 21 or 28 after 4-HT application. Mice were monitored for another 8 weeks after surgery for the appearance of metastatic tumors.

Figure S3: Transcriptome analysis in primary, metastatic tumors and CTCs (A) Genes upregulated in metastatic tumor compared with the matched primary tumor were intersected across different mice (n = 4, from mice BP-53, BP-55, BP-72 and BP-73). Minimal overlap of genes was found in this comparison. (B) Similarly, genes downregulated in metastatic lesions compared with the primary tumor also displayed minimal overlap across the same 4 samples. (C-F) Hoshida liver carcinoma gene set was significantly enriched in CTCs. Hoshida gene signature was found to be overrepresented not only in CTC-enriched genes (genes upregulated by >2-fold in Chip-enriched cells compared with mock-enriched cells, C and E) but also in CTC-specific genes (CTC-enriched genes specifically overexpressed by >2-fold compared to the primary tumor, D and F). (G) Expression of MITF is lower in CTCs. Compared to normal melanocytes and primary tumor cells, CTCs express lower level of MITF (n= 4, from mice BP-53, BP-55, BP-72 and BP-73; rpm, reads per million).

Figure S4: Optimization of melanoma ^{HB}CTC-Chip for patient. (A) A list of candidate antigens tested for human ^{HB}CTC-Chip. Top panel, melanoma cell surface markers intended for both CTC immunoaffinity isolation and subsequent immunofluorescence (IF)-based CTC identification. Bottom panel, cytoplasmic or nuclear antigens intended for IF-based CTC detection only. Bold, antigens chosen for CTC applications; asterisk, antigens used for both CTC capture and IF detection (note: regarding such antigens, distinct antibodies were used). (B) IF staining of melanoma cell lines, SK-MEL-28 and UACC62, using CTC detection antibody cocktail (red, detection antibody staining; blue, DAPI nuclear staining). Differential expression of melanoma antigens was evident in the two cell lines. (C-E). Combinatorial uses of capture antibodies improved CTC capture efficiency. (C) SK-MEL-28 expresses CSPG4 (blue peak), p97 (green peak) and MCAM (orange peak) at different levels as determined by flowcytometry. (D) More than 90% of SK-MEL-28 cells were recovered on ^{HB}CTC-Chip with an antibody cocktail against CSPG4/MCAM/P97 compared to CSPG4/MCAM or CSPG4 alone (total amount of antibody on each ^{HB}CTC-Chip was 10ug equally split between different antibodies). (E) Increased CTC yield (>2-fold) from patient blood (M5) was observed when MCAM was incorporated into the capture antibody cocktail (total antibody on each chip was 10ug; CSPG4/MCAM/P97-1 and CSPG4/MCAM/P97-2 represent two ^{HB}CTC-Chips serving as technical replicates). (F) Representative images of a patient CTC cluster (M6). DAPI, blue; MEL, red; scale bar, 10μm.

Figure S1: Characterization of mouse melanoma and CTCs. (Related to Figure 1)

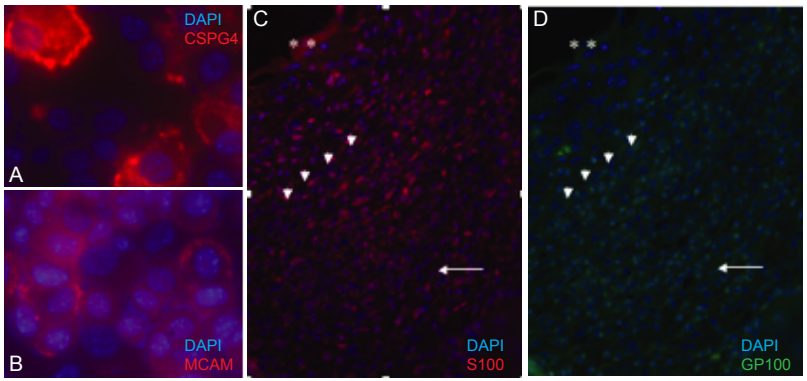

E

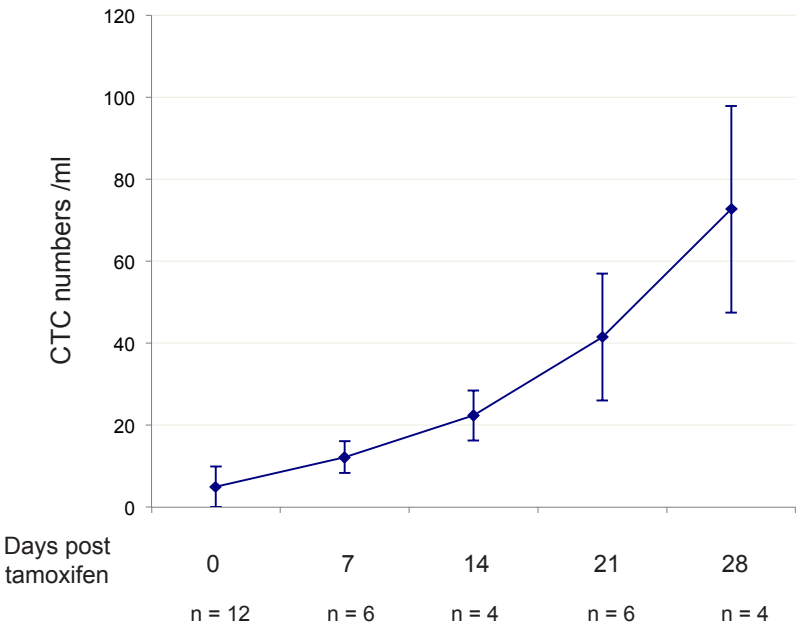

F

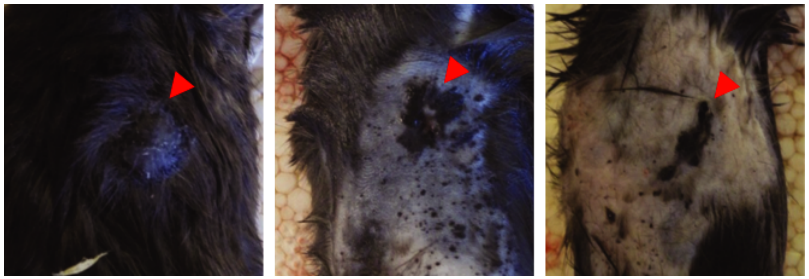

G

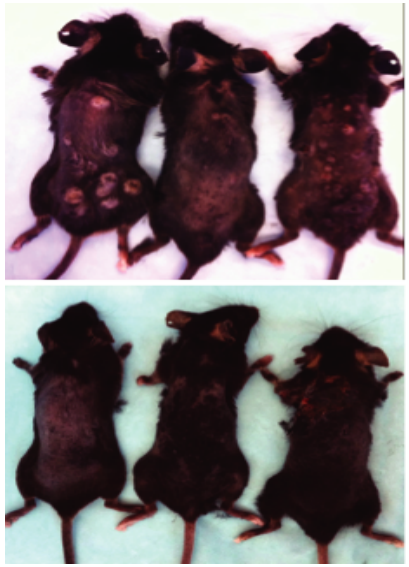

H

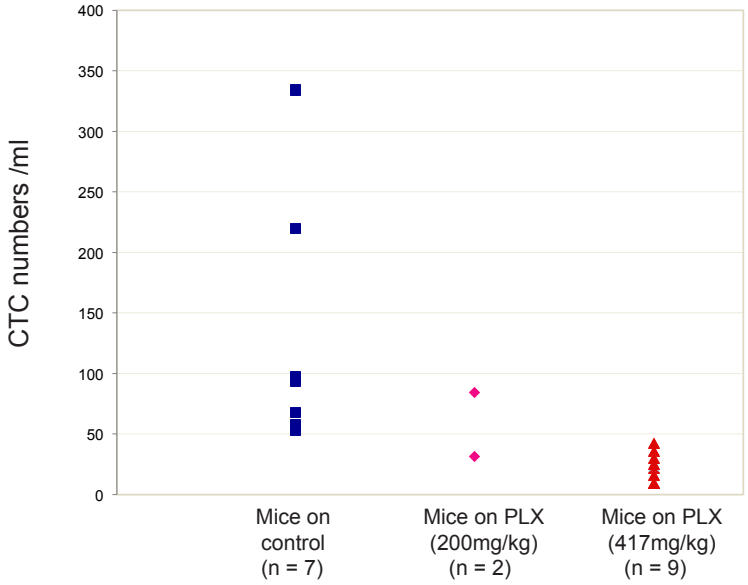

Figure S2: Mouse melanoma surgery model. (Related to Figure 2)

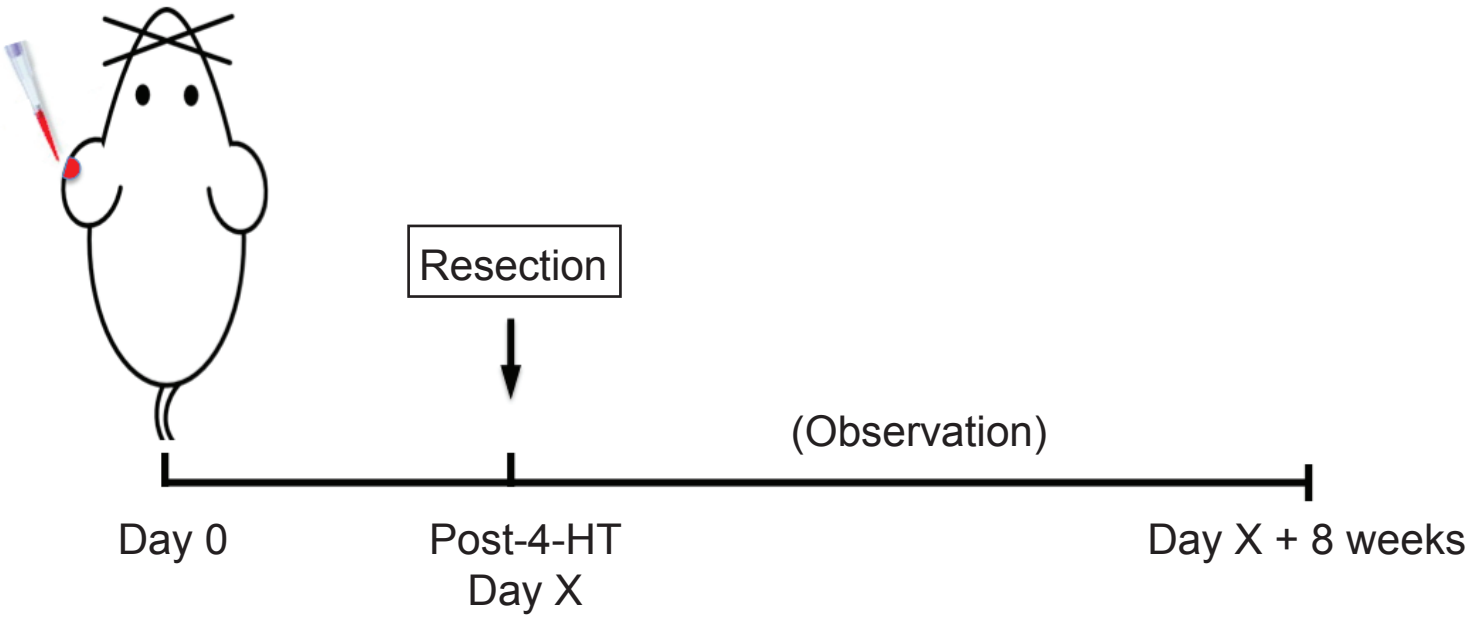

Resection post 4-HT (days)	Mice with met. tumor/total mice
7	11/11
14	7/7
21	5/5
28	3/3

Figure S3: Data analyses of the RNA-Sequencing experiment. (Related to Figure 3)

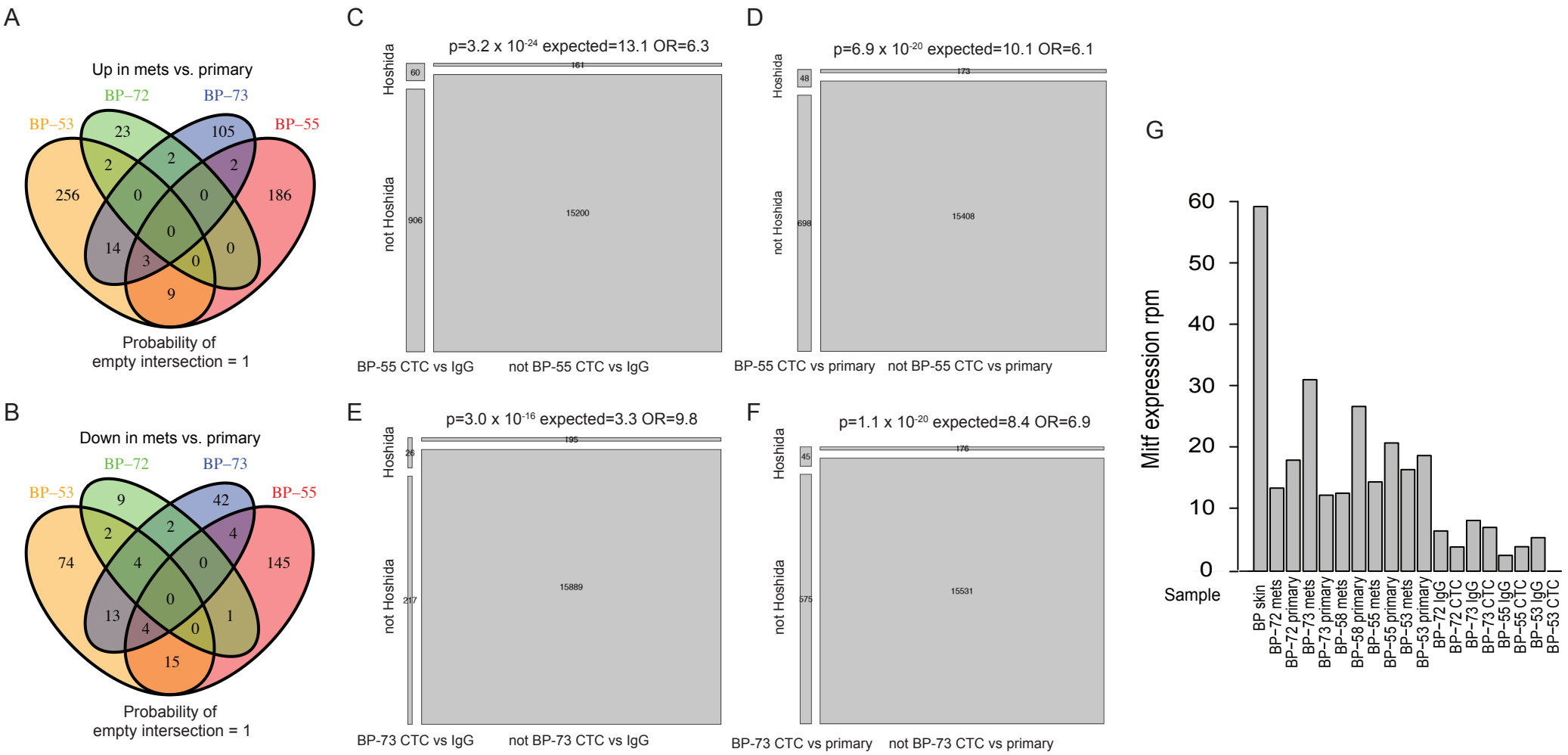

Figure S4: The construction and optimization of ^{HB}CTC-Chip for patient CTC enrichment. (Related to Figure 4)

A

Cell Surface Markers					
A2B5	**CD90**	**CD117**	**c-Met**	**CSPG4***	**EGFR**
EPHA2	**HNK-1**	**MCAM***	**NCad**	**NGFR**	**P97**
CD63	CDH19	ERBB2	ERBB3	GD2	GD3
KCad	O1	O4			

Cytoplamsic/nuclear markers					
aSMA	**TYRP-1**	GalNAc-T	GP100	MageA	MAP2
MelanA	MITF	NESTIN	Pax3	PIAS3	PRAME
S100	SOX2	SOX9	SOX10	SLUG	SNAIL
TYRP-2	TUJ1	TYR			

B

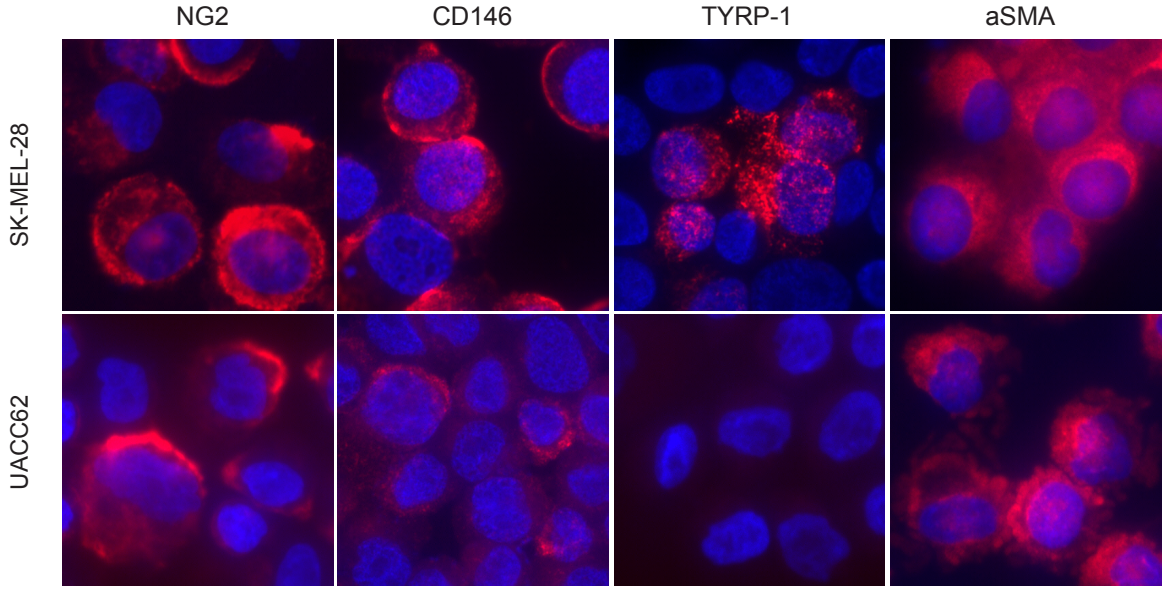

C

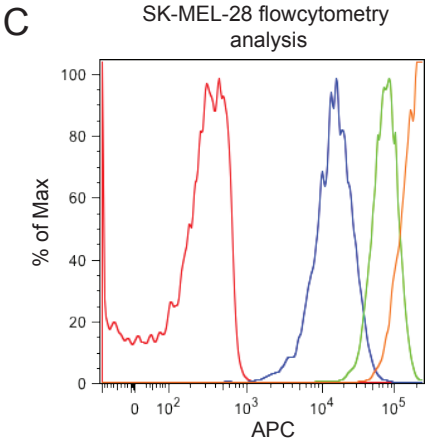

D

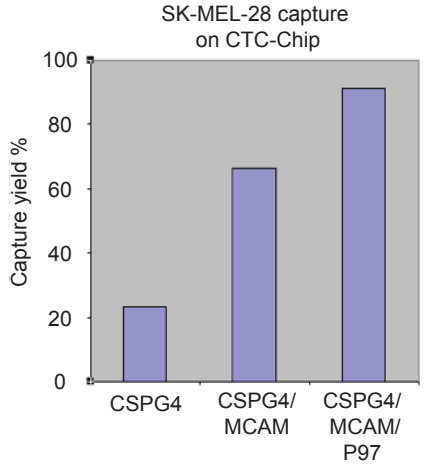

E

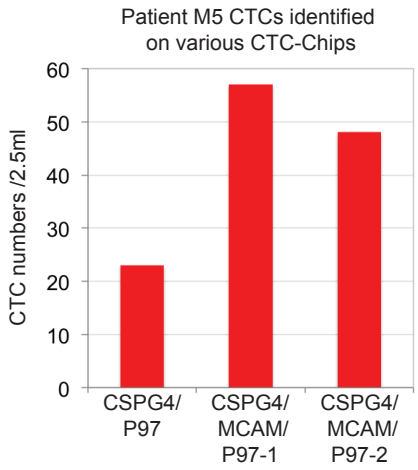

F

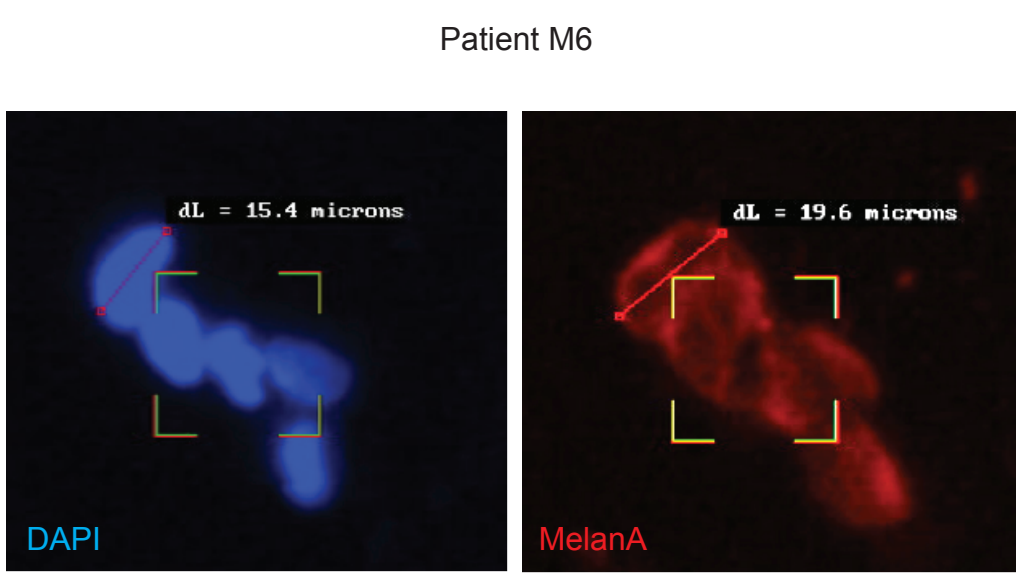

Table S1: Histological analysis of early mouse tumors. (Related Figure 2)

Mouse ID	BP154	BP156	BP157	BP160	BP161	BP162	BP163	BP164	BP167	BP168	BP177	BP178
CTC counts /ml	73.8889	50.0588	61.2222	68	48.5556	46.4444	86.5556	120	41.4	50.4	54.4	86.95
Tumor thickness (mm)	0.2	0.12	0.13	0.27	0.12	0.13	0.2	0.27	0.12	0.11	0.17	0.2
Ulceration	absent	absent	absent	absent	absent	absent	absent	absent	absent	absent	absent	absent
Fat involvement	present	present	present	present	present	present	present	present	present	present	present	present
Invading cartilage	absent	absent	absent	absent	absent	absent	absent	absent	absent	absent	absent	absent
Spindle morphology	absent	absent	absent	absent	absent	absent	absent	absent	absent	absent	absent	absent
Epithelioid morphology	present	present	present	present	present	present	present	present	present	present	present	present
Neural differentiation	absent	absent	absent	absent	absent	absent	absent	absent	absent	absent	absent	absent
Marked pigmentation	present	present	present	present	present	present	present	present	present	present	present	present
Mitoses per squared millimeter	0	0	0	0	0	0	0	0	0	0	0	0
Necrosis	absent	absent	absent	absent	absent	absent	absent	absent	absent	absent	absent	absent
Dermal hyalinization/fibrosis	absent	absent	absent	absent	absent	absent	absent	absent	absent	absent	absent	absent

Table S2: Gene Ontology (GO) analysis on CTC-enriched genes. (Related to Figure 3)

Top 10 functional Categories of CTC-enriched genes			
Functional Categories	Number of genes	Number of genes expected	P-Value
Lysosome	15	1.6	6.57×10^{-11}
Plasma membrane	62	29	1.18×10^{-09}
Inflammatory response	15	2.3	1.32×10^{-08}
Protein binding	104	67.1	1.67×10^{-08}
Extracellular region	40	16.6	1.22×10^{-07}
Immune response	15	3	3.66×10^{-07}
Signal transduction	30	11.3	7.70×10^{-07}
Cellular component movement	9	1	9.37×10^{-07}
External side of plasma membrane	10	1.4	1.42×10^{-06}
Melanosome	8	1	5.20×10^{-06}

Table S3: Selected list of CTC genes. (Related to Figure 3)

Supplemental Table 2: Selected list of genes expressed in CTCs		
Gene	Description	Function
Tgfbi	Transforming growth factor, beta induced	TGFbeta signaling
Mafb	V-maf musculoaponeurotic fibrosarcoma oncogene family, protein B (avian)	
Bak1	BCL2-antagonist/killer 1	
Api5	Apoptosis inhibitor 5	
Fn1	Fibronectin 1	EMT marker
Tgfb1	Transforming growth factor, beta 1	TGFbeta signaling
Zeb2	Zinc finger E-box binding homeobox 2	EMT inducer
Cd44	CD44 antigen	
Lyn	Yamaguchi sarcoma viral (v-yes-1) oncogene homolog	
Klf6	Kruppel-like factor 6	Stem cell differentiation, Klf family member
Vim	Vimentin	EMT marker
App	Amyloid beta (A4) precursor protein	
Klf4	Kruppel-like factor 4 (gut)	Stem cell reprogramming
Akt1	Thymoma viral proto-oncogene 1	
Arpc5	Actin related protein 2/3 complex, subunit 5	
Arpc2	Actin related protein 2/3 complex, subunit 2	
Ceacam1	Carcinoembryonic antigen-related cell adhesion molecule 1	CD66a membrane antigen
Sbno2	Strawberry notch homolog 2 (Drosophila)	Positive regulator of EGF/RAS
Hsp90b1	Heat shock protein 90, beta (Grp94), member 1	
Diap1	Diaphanous homolog 1 (Drosophila)	Microtubule rearrangement, Neuron migration
Zic1	Zinc finger protein of the cerebellum 1	
Wipf1	WAS/WASL interacting protein family, member 1	
Zyx	Zyxin	Tgfb induced cell movement
Rhoa	Ras homolog gene family, member A	Cell motility
Ssh2	Slingshot homolog 2 (Drosophila)	Actin dynamics
S100a6	S100 calcium binding protein A6 (calcyclin)	
Tgfbr1	Transforming growth factor, beta receptor I	
Neurl3	Neuralized homolog 3 homolog (Drosophila)	Notch signaling
Snord35a	small nucleolar RNA, C/D box 35A	
Snord33	small nucleolar RNA, C/D box 33	
Snora70	Small nucleolar RNA, H/ACA box 70	
Glipr2	GLI pathogenesis-related 2	Tgfb/SHH signaling pathway downstream
Akt2	Thymoma viral proto-oncogene 2	
Pum2	Pumilio 2 (Drosophila)	mRNA translation regulation
Hif1a	Hypoxia inducible factor 1, alpha subunit	Hypoxia
Tgfbr2	Transforming growth factor, beta receptor II	
Myc	Myelocytomatosis oncogene	
Fli1	Friend leukemia integration 1	ETS transcription factor
Itch	Itchy, E3 ubiquitin protein ligase	
Cic	Capicua homolog (Drosophila)	granule neuron development
Notch2	Notch gene homolog 2 (Drosophila)	Notch signaling
Brpf1	Bromodomain and PHD finger containing, 1	
Rock2	Rho-associated coiled-coil containing protein kinase 2	
Ets1	E26 avian leukemia oncogene 1, 5' domain	
Hsp90ab1	Heat shock protein 90 alpha (cytosolic), class B member 1	
Qk	Quaking	CNS development
Stat6	Signal transducer and activator of transcription 6	
Ezr	Ezrin	
Malat1	Metastasis associated lung adenocarcinoma transcript 1 (non-coding RNA)	Non-coding lincRNA
Tet2	Tet oncogene family member 2	
Vav1	Vav 1 oncogene	
Spnb2	Spectrin beta 2	
Stat3	Signal transducer and activator of transcription 3	
Jak1	Janus kinase 1	
Ewsr1	Ewing sarcoma breakpoint region 1	
Kdm2a	Lysine (K)-specific demethylase 2A	
Nras	Neuroblastoma ras oncogene	
Hsp90aa1	Heat shock protein 90, alpha (cytosolic), class A member 1	
Sbno1	Sno, strawberry notch homolog 1 (Drosophila)	
Kdm6b	KDM1 lysine (K)-specific demethylase 6B	
Pten	Phosphatase and tensin homolog	
Msi2	Musashi homolog 2 (Drosophila)	NSC, HSC proliferation/differentiation
Cnr1	Cannabinoid receptor 1 (brain)	
Sp1	Trans-acting transcription factor 1	
Msl2	Male-specific lethal 2 homolog (Drosophila)	
Klf2	Kruppel-like factor 2 (lung)	Klf family member

Table S4: List of antibodies used in melanoma patient CTC enrichment and identification. (Related to Figure 4)

Antibodies used for melanoma CTC capture			
Antigen	Clone	Isotype	Reference
CSPG4	LHM-2	Mouse IgG1	Kupsch et al. (1995)
Melanotransferrin/P97	L-235	Mouse IgG1	Houghton et al. (1982)
MCAM	P1H12	Mouse IgG1	Denton et al. (1992); Solovey et al. (1997)
CD117	104D2	Mouse IgG1	Ohashi et al. (1996) Rappold et al. (1997)
NGFR	NGFR5	Mouse IgG1	Boiko et al. (2010) Thompson et al. (1989)
N-Cadherin	8C11	Mouse IgG1	Puch et al. (2001)
EGFR	Certuximab	Chimeric	Hoek et al. (2008) Prewett et al. (1996)
EphA2		Goat polyclonal	Udayakumar et al. (2011)
CD90	5E10	Mouse IgG	Winnepenninckx et al. (2003)
c-Met		Goat polyclonal	Natali et al. (1993)
A2B5	105	Mouse IgM	Eisenbarth et al. (1979); Yamamura and Mishima (1990)
HNK-1	HNK-1	Mouse IgM	Schachner and Martini (1995); Tang et al. (1996)
Antibodies used for melanoma CTC detection by IF			
Antigen	Clone	Isotype	Reference
CSPG4	9.2.27	Mouse IgG2a	Morgan et al. (1981)
MCAM	SHM-57	Mouse IgG2a	
TYRP-1	TA99	Mouse IgG2a	Thomson et al. (1985)
alpha-SMA	1A4	Mouse IgG2a	Banerjee et al. (1996) Dundr et al. (2009) (Supplemental figure 1)

SUPPLEMENTAL REFERENCES

Banerjee, S. S., Bishop, P. W., Nicholson, C. M., and Eyden, B. P. (1996). Malignant melanoma showing smooth muscle differentiation. Journal of clinical pathology *49*, 950-951.

Boiko, A. D., Razorenova, O. V., van de Rijn, M., Swetter, S. M., Johnson, D. L., Ly, D. P., Butler, P. D., Yang, G. P., Joshua, B., Kaplan, M. J.*, et al.* (2010). Human melanoma-initiating cells express neural crest nerve growth factor receptor CD271. Nature *466*, 133-137.

Dankort, D., Curley, D. P., Cartlidge, R. A., Nelson, B., Karnezis, A. N., Damsky, W. E., Jr., You, M. J., DePinho, R. A., McMahon, M., and Bosenberg, M. (2009). Braf(V600E) cooperates with Pten loss to induce metastatic melanoma. Nat Genet *41*, 544-552.

Denton, K. J., Stretch, J. R., Gatter, K. C., and Harris, A. L. (1992). A study of adhesion molecules as markers of progression in malignant melanoma. J Pathol *167*, 187-191.

Dundr, P., Povysil, C., and Tvrdik, D. (2009). Actin expression in neural crest cell-derived tumors including schwannomas, malignant peripheral nerve sheath tumors, neurofibromas and melanocytic tumors. Pathol Int *59*, 86-90.

Eisenbarth, G. S., Walsh, F. S., and Nirenberg, M. (1979). Monoclonal antibody to a plasma membrane antigen of neurons. Proc Natl Acad Sci of U S A *76*, 4913-4917.

Hoek, K. S., Eichhoff, O. M., Schlegel, N. C., Dobbeling, U., Kobert, N., Schaerer, L., Hemmi, S., and Dummer, R. (2008). In vivo switching of human melanoma cells between proliferative and invasive states. Cancer Res *68*, 650-656.

Houghton, A. N., Eisinger, M., Albino, A. P., Cairncross, J. G., and Old, L. J. (1982). Surface antigens of melanocytes and melanomas. Markers of melanocyte differentiation and melanoma subsets. J Exp Med *156*, 1755-1766.

Kupsch, J. M., Tidman, N., Bishop, J. A., McKay, I., Leigh, I., and Crowe, J. S. (1995). Generation and selection of monoclonal antibodies, single-chain Fv and antibody fusion phage specific for human melanoma-associated antigens. Melanoma Res *5*, 403-411.

Morgan, A. C., Jr., Galloway, D. R., and Reisfeld, R. A. (1981). Production and characterization of monoclonal antibody to a melanoma specific glycoprotein. Hybridoma *1*, 27-36.

Natali, P. G., Nicotra, M. R., Di Renzo, M. F., Prat, M., Bigotti, A., Cavaliere, R., and Comoglio, P. M. (1993). Expression of the c-Met/HGF receptor in human melanocytic neoplasms: demonstration of the relationship to malignant melanoma tumour progression. Br J Cancer *68*, 746-750.

Ohashi, A., Funasaka, Y., Ueda, M., and Ichihashi, M. (1996). c-KIT receptor expression in cutaneous malignant melanoma and benign melanotic naevi. Melanoma Res *6*, 25-30.

Prewett, M., Rockwell, P., Rockwell, R. F., Giorgio, N. A., Mendelsohn, J., Scher, H. I., and Goldstein, N. I. (1996). The biologic effects of C225, a chimeric monoclonal antibody to the EGFR, on human prostate carcinoma. J Immunother Emphasis Tumor Immunol *19*, 419-427.

Puch, S., Armeanu, S., Kibler, C., Johnson, K. R., Muller, C. A., Wheelock, M. J., and Klein, G. (2001). N-cadherin is developmentally regulated and functionally involved in early hematopoietic cell differentiation. J Cell Sci *114*, 1567-1577.

Rappold, I., Ziegler, B. L., Kohler, I., Marchetto, S., Rosnet, O., Birnbaum, D., Simmons, P. J., Zannettino, A. C., Hill, B., Neu, S.*, et al.* (1997). Functional and phenotypic

characterization of cord blood and bone marrow subsets expressing FLT3 (CD135) receptor tyrosine kinase. Blood *90*, 111-125.
Schachner, M., and Martini, R. (1995). Glycans and the modulation of neural-recognition molecule function. Trends Neurosci *18*, 183-191.
Solovey, A., Lin, Y., Browne, P., Choong, S., Wayner, E., and Hebbel, R. P. (1997). Circulating activated endothelial cells in sickle cell anemia. N Engl J Med *337*, 1584-1590.
Stott, S. L., Hsu, C. H., Tsukrov, D. I., Yu, M., Miyamoto, D. T., Waltman, B. A., Rothenberg, S. M., Shah, A. M., Smas, M. E., Korir, G. K.*, et al.* (2010). Isolation of circulating tumor cells using a microvortex-generating herringbone-chip. Proc Natl Acad Sci U S A *107*, 18392-18397.
Tang, N. E., Luyten, G. P., Mooy, C. M., Naus, N. C., de Jong, P. T., and Luider, T. M. (1996). HNK-1 antigens on uveal and cutaneous melanoma cell lines. Melanoma Res *6*, 411-418.
Thompson, S. J., Schatteman, G. C., Gown, A. M., and Bothwell, M. (1989). A monoclonal antibody against nerve growth factor receptor. Immunohistochemical analysis of normal and neoplastic human tissue. Am J Clin Pathol *92*, 415-423.
Thomson, T. M., Mattes, M. J., Roux, L., Old, L. J., and Lloyd, K. O. (1985). Pigmentation-associated glycoprotein of human melanomas and melanocytes: definition with a mouse monoclonal antibody. J Invest Dermatol *85*, 169-174.
Udayakumar, D., Zhang, G., Ji, Z., Njauw, C. N., Mroz, P., and Tsao, H. (2011). EphA2 is a critical oncogene in melanoma. Oncogene *30*, 4921-4929.
Winnepenninckx, V., De Vos, R., Stas, M., and van den Oord, J. J. (2003). New phenotypical and ultrastructural findings in spindle cell (desmoplastic/neurotropic) melanoma. Appl Immunohistochem Mol Morphol *11*, 319-325.
Yamamura, K., and Mishima, Y. (1990). Antigen dynamics in melanocytic and nevocytic melanoma oncogenesis: anti-ganglioside and anti-ras p21 antibodies as markers of tumor progression. J Invest Dermatol *94*, 174-182.
Yu, M., Ting, D. T., Stott, S. L., Wittner, B. S., Ozsolak, F., Paul, S., Ciciliano, J. C., Smas, M. E., Winokur, D., Gilman, A. J.*, et al.* (2012). RNA sequencing of pancreatic circulating tumour cells implicates WNT signalling in metastasis. Nature *487*, 510-513.